Defect and Diffusion Forum
ISSN: 1662-9507, Vol. 451, pp 133-146
doi:10.4028/p-jEnO27
© 2026 The Author(s). Published by Trans Tech Publications Ltd, Switzerland.
Submitted: 2026-01-19
Revised: 2026-02-25
Accepted: 2026-03-01
Online: 2026-04-17

Multi-Objective Optimization of Injection-Molded Components for Defect Reduction and Warpage Minimization

Keltoum Oubellaouch[1,2,a*], Riccardo Pelaccia[1,b], Giulia Zaniboni[1,2,c], Vincenzina Siciliani[1,d] and Barbara Reggiani[1,3,e]

[1]DISMI Department of Sciences and Methods for Engineering – University of Modena and Reggio Emilia, Via Amendola 2, 42122, Reggio Emilia, Italy

[2]INTERMECH, University of Modena and Reggio Emilia, Italy

[3]EN&TECH, University of Modena and Reggio Emilia, Italy

[a]keltoum.oubellaouch@unimore.it, [b]riccardo_p@unimore.it , [c]giulia.zaniboni@unimore.it, [d]vincenzina.siciliani@unimore.it, [e]barbara.reggiani@unimore.it

Keywords: Injection Molding, Optimization, Numerical Simulation, Warpage Reduction.

Abstract. Warpage in injection-molded thin-walled box-shaped parts is primarily caused by non-uniform cooling and differential shrinkage. This study proposes a two-step, multi-objective optimization strategy to reduce part warpage by addressing both thermal and geometric factors. In the first step, the mold cooling system is optimized through a bi-objective formulation that simultaneously minimizes (i) the temperature standard deviation within the part and (ii) the total cooling channel length. The optimization is carried out using a coupled workflow involving parametric CAD modeling, Autodesk Moldflow simulations, and a genetic algorithm. The optimized cooling design reduces temperature non-uniformity by 44% compared to a conventional cooling layout. In the second step, a geometric optimization is performed through the addition of a reinforcing border, where maximum deflection and total part volume are minimized simultaneously. The combined optimization leads to a reduction in maximum warpage from 14.5 mm in the reference configuration to 2.06 mm in the final design. The results demonstrate the effectiveness of a sequential optimization approach in achieving significant warpage reduction while maintaining material and manufacturing efficiency.

Introduction

Warpage is widely recognized as one of the most critical quality defects in plastic injection molding, especially for thin-walled and box-shaped components, where differential cooling, non-uniform shrinkage, and residual stress development lead to significant geometric distortions [1]. The defect originates from the intrinsic complexity of the injection molding process, in which the polymer melt experiences strongly coupled thermal, mechanical, and rheological phenomena during filling, packing, and cooling stages [2]. Spatial variations in temperature and pressure, together with molecular orientation effects, result in uneven volumetric contraction across the part thickness and along its geometry, ultimately causing warpage upon ejection from the mold [3,4]. Due to this strong coupling and nonlinearity, empirical or trial-and-error approaches based on operator experience are often insufficient to guarantee consistent part quality, particularly for geometries with stringent dimensional tolerances [5].

To address these limitations, numerical simulation has become a central tool for predicting warpage and supporting process and design decisions in injection molding. Finite-element-based simulation environments allow the coupled analysis of melt flow, heat transfer, solidification, and residual stress evolution, providing a physically consistent framework for understanding warpage formation mechanisms [6]. Advanced numerical models have further improved prediction accuracy by accounting for three-dimensional effects and material anisotropy, as demonstrated in studies on fiber-reinforced polymers, where orientation-dependent thermo-mechanical behavior plays a dominant role in warpage development [1,7]. Simulation-driven approaches therefore enable the

This article is an open access article under the terms and conditions of the Creative Commons Attribution (CC BY) license (https://creativecommons.org/licenses/by/4.0)

evaluation of warpage prior to mold manufacturing, significantly reducing development time and cost [2].

Building upon numerical simulation capabilities, a substantial body of research has focused on the optimization of injection molding process parameters to minimize warpage. Widely adopted approaches rely on design of experiments (DOE), including Taguchi and orthogonal array methods, to identify influential parameters and their optimal combinations [8,9]. While these techniques are computationally efficient and easy to implement, they are inherently limited to discrete parameter levels and typically provide optimal solutions only within a predefined experimental space [8]. As a result, they may fail to capture the true global optimum in highly nonlinear problems such as warpage control.

To overcome these limitations, advanced optimization strategies based on evolutionary algorithms and numerical optimization frameworks have been increasingly applied. Genetic algorithms, particle swarm optimization, and multi-objective optimization techniques have been combined with injection molding simulations to systematically explore large design spaces and reduce warpage [10,11]. In many cases, these approaches have demonstrated superior performance compared to classical DOE methods, particularly when multiple interacting parameters must be optimized simultaneously. However, the computational cost associated with repeated high-fidelity simulations remains a major challenge.

To mitigate this issue, surrogate-based optimization approaches have been widely adopted. Artificial neural networks, response surface methodologies, and Kriging models are commonly used to construct approximate relationships between process parameters and warpage response, replacing expensive numerical simulations during the optimization loop [12,13]. These surrogate models are often coupled with global optimization algorithms, enabling efficient exploration of the design space. Nevertheless, several studies emphasize that surrogate model accuracy is strongly dependent on the quality and size of the training dataset, and that insufficient sampling may lead to unreliable predictions, particularly in the presence of strong nonlinear thermo-mechanical interactions [12,13].

Despite the increasing sophistication of optimization methodologies, many studies still adopt single-objective formulations, typically focusing exclusively on minimizing warpage magnitude [8–10]. While such approaches may yield numerically optimal solutions, they often neglect practical considerations related to manufacturability, mold complexity, and industrial robustness. More recent works have introduced multi-objective optimization frameworks to address trade-offs between warpage, shrinkage, and cycle time [11]. However, even within these frameworks, the selected objectives are frequently limited to final deformation metrics, without explicitly addressing the physical mechanisms responsible for warpage formation.

Among the various influencing factors, the cooling phase has consistently been identified as a dominant contributor to warpage. Cooling accounts for the largest portion of the injection molding cycle time and plays a decisive role in determining temperature gradients within the molded part [14]. The design of the cooling system, including channel layout, distance from the cavity surface, and coolant conditions, directly affects heat removal efficiency and temperature uniformity. Consequently, significant research efforts have focused on optimizing cooling system design, with particular attention given to conformal cooling channels enabled by additive manufacturing technologies [14,15]. These studies demonstrate that improved cooling performance can significantly reduce warpage and residual stresses while also decreasing cycle time.

Nevertheless, most cooling system optimization studies evaluate performance using global indicators such as maximum temperature, cooling time, or final warpage value [14,15]. While these metrics are useful from an operational standpoint, they do not explicitly quantify the spatial uniformity of the temperature field within the part. Only a limited number of works acknowledge the importance of temperature uniformity, and even fewer treat it as a primary optimization objective [14]. This represents a significant gap in the literature, considering that warpage fundamentally arises from spatial temperature gradients and the resulting differential shrinkage during cooling [1,12].

From a physical perspective, temperature homogenization during cooling constitutes a direct and meaningful indicator of warpage propensity. Uneven temperature distributions lead to localized

differences in solidification rate and volumetric contraction, generating residual stresses that are released upon ejection [5,12]. Despite this well-established mechanism, optimization formulations rarely incorporate temperature dispersion metrics—such as the standard deviation of the temperature field—as explicit objective functions. Addressing this limitation is essential to establish a clearer and more physically consistent link between cooling system design, thermal behavior, and final part quality.

In this context, the present work proposes an integrated multi-objective optimization framework in which the CAD environment (Fusion 360) is coupled with the process simulation module (Autodesk Moldflow Insight) through an optimization platform. A two-step, simulation-driven strategy is adopted: first, the cooling system is optimized by explicitly minimizing temperature non-uniformity within the part while limiting cooling system complexity; subsequently, a geometry-based optimization is performed to further reduce warpage through the introduction of a reinforcing border. All optimization activities are carried out using direct numerical simulations within an optimization platform a physically consistent relationship between cooling system design, temperature distribution, and final part quality.

Materials and Methods

In this work, a two-step optimization procedure was developed to mitigate warpage in a thin-walled polymer component by addressing both thermal and geometric contributors. The investigated part is a box-shaped component with overall dimensions of 300 mm × 200 mm × 150 mm and a uniform wall thickness of 4 mm. For this class of components, warpage is primarily driven by differential cooling between the inner and outer surfaces, which results in non-uniform shrinkage during the cooling phase. Consequently, the first step of the proposed methodology focuses on the optimization of the mold cooling system with the objective of achieving the most uniform temperature distribution within the part. This first step is formulated as a bi-objective optimization problem, in which temperature uniformity and cooling system complexity are minimized simultaneously. Once the optimal cooling configuration is identified, a second optimization step is carried out to further reduce warpage through a geometric modification of the component, consisting of the addition of a reinforcing border to the box. In this second step, the optimization procedure aims to determine the most suitable border configuration to minimize the final deformation while preserving the overall part geometry. Similarly, this second stage is also formulated as a bi-objective optimization problem, where deformation reduction and material usage are simultaneously considered in order to achieve a balanced structural solution. All optimization activities are performed using an optimization platform, which is employed to manage the workflow, execute simulations, and evaluate the defined objective functions.

Step 1: Cooling System Optimization. The first step of the optimization procedure concerns the design of the mold cooling system. The mold configuration corresponds to a single-cavity, two-plate mold. Within this configuration, three distinct cooling planes are considered. The first cooling plane, referred to as *Cooling Plane 1* in Figure 1, is located in the fixed plate of the mold and consists of six straight cooling channels oriented along the *y*-axis. The second cooling plane (*Cooling Plane 2* in Figure 1) is positioned at a *z*-coordinate corresponding to the mid-height of the box-shaped component. The third cooling plane (*Cooling Plane 3* in Figure 1) is located in the moving plate of the mold and plays a key role in the thermal management of the part. This plane allows the integration of baffles extending toward the depth of the box, enabling enhanced heat extraction from the inner regions of the component. The inclusion of these baffles is particularly important for reducing the thermal gradient between the inner and outer surfaces of the box, thereby promoting a more uniform temperature distribution during the cooling phase.

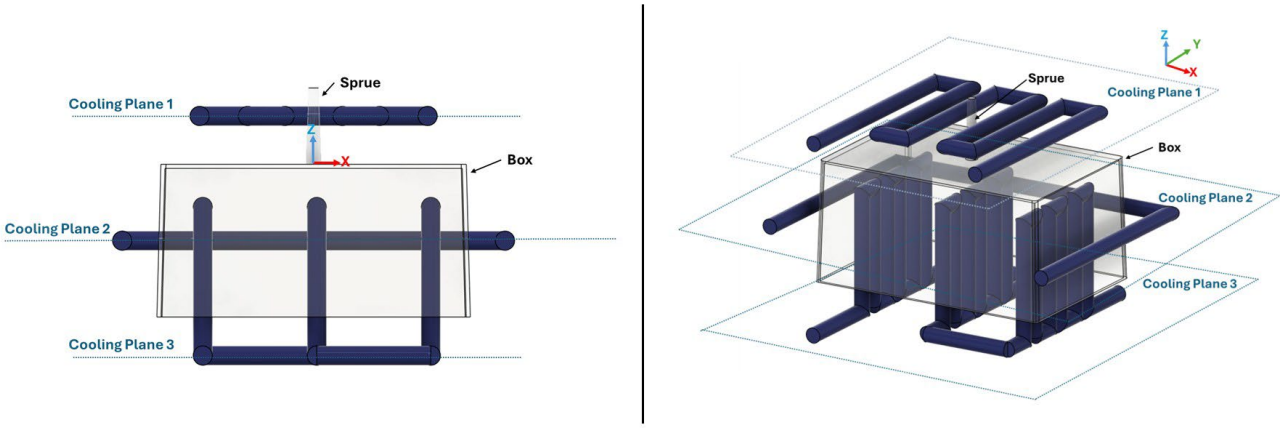

Fig.1 Schematic of the single-cavity, two-plate mold showing the three cooling planes

Within the cooling system optimization, several design parameters could, in principle, be varied. However, in order to limit the complexity of the optimization problem and ensure a manageable design space, a reduced set of design variables was selected. The first design variable is the diameter of the cooling channels, denoted as *"d_c"*, which was allowed to vary between 8 mm and 20 mm. The second variable defines the distance between Cooling Plane 1 and the box-shaped part. This distance was parameterized as the product of a dimensionless factor *"a"* and the channel diameter "d_c", with the factor *"a"* constrained to the range 1–2.5. Finally, the third design variable is the number of branches, *"n_1"*, corresponding to the number of cooling channels oriented parallel to the *y*-direction from which baffles are introduced in the moving plate. The number of branches was varied between 3 and 8, while the number of baffles per branch was kept constant and set equal to three for all configurations.

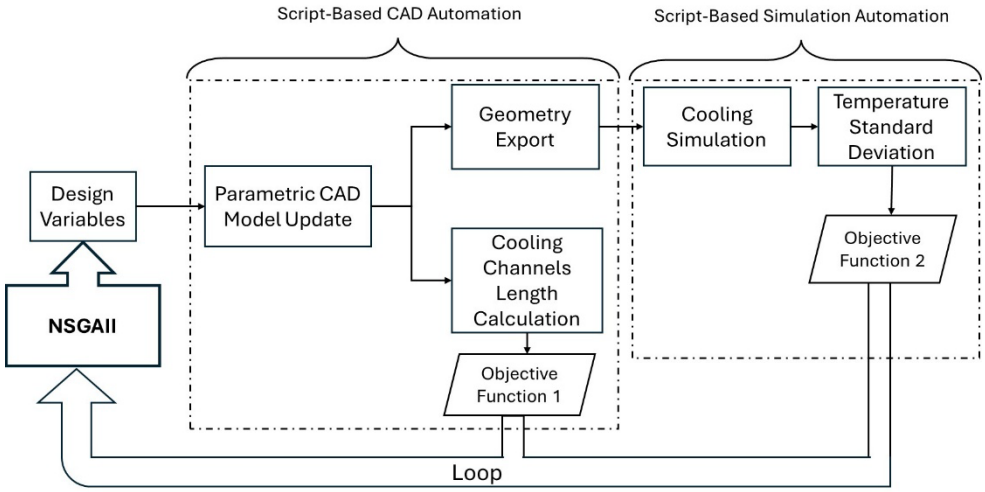

Fig. 2 Workflow of the first optimization procedure (Step 1: Cooling System Optimization)

The objective of the first optimization step is twofold. The primary objective is the reduction of temperature non-uniformity within the molded part, which is quantified by minimizing the standard deviation of the temperature field over the volume of the box. The objective function associated with thermal uniformity is defined as (Eq. 1):

$$f_1 = \sigma_T = \sqrt{\frac{1}{N}\sum_{i=1}^{N}(T_i - \bar{T})} \quad (1)$$

where T_i represents the temperature at the i^{th} evaluation point within the part, $\bar{T}$ is the average temperature, and N is the total number of sampled points.

In parallel, a second objective is introduced to limit the overall complexity of the cooling system by minimizing the total length of the cooling channels, L_{tot}. This objective accounts for practical manufacturing and structural considerations. While an extensive cooling network with large channel diameters and a high number of baffles can significantly enhance heat extraction and temperature uniformity, it may also compromise mold mechanical integrity by excessive material removal and increase machining complexity and cost. Therefore, the optimization seeks a balanced solution that achieves the highest possible temperature uniformity with the minimum necessary cooling system length. The second objective function is thus expressed as (Eq. 2):

$$f_2 = L_{tot} \tag{2}$$

The combined optimization framework enables the identification of cooling system configurations that provide an effective thermal performance while remaining compatible with mold strength and manufacturing constraints.

The cooling system optimization problem was solved using a commercial optimization platform. Figure 2 illustrates the complete workflow implemented for Step 1. The workflow integrates parametric CAD modeling, numerical simulation, and multi-objective optimization in an automated loop. At the top level of the workflow, the design variables—namely the number of branches n_1, the cooling channels diameter d_c, and the distance factor a—are defined and controlled by the optimization algorithm. The original Non-dominated Sorting Genetic Algorithm II (NSGA-II) was selected to solve the multi-objective optimization problem. The algorithm was configured with an initial Design of Experiments (DOE) consisting of 20 configurations, followed by 50 generations, resulting in a total of 1000 evaluated designs. The coupling between the optimization platform and Autodesk Fusion 360 was implemented through an automated script-based interface, where the required commands were executed using Windows batch scripting. For each iteration, the optimization algorithm generates a new set of design variables, which are automatically assigned to the parametric CAD model. The procedure begins by opening an existing Fusion 360 project containing a fully parametric CAD model of the cooling system, where the design variables are defined as editable parameters. Once the design variables are updated, Fusion 360 regenerates the cooling system geometry and exports the corresponding CAD model in STEP format. Subsequently, the total length of the cooling channels is automatically computed and written to an output file. This value is then retrieved by the optimization platform and stored as an output variable directly associated with the objective function representing the total cooling system length. The numerical simulation of the cooling process was performed using Autodesk Moldflow Insight, which was interfaced with the optimization platform through an automated script-based coupling mechanism implemented using Visual Basic scripting. The execution of Moldflow was conditioned on the successful generation of the STEP file by Fusion 360. Once launched, Moldflow imports the current cooling system geometry as CAD data. A three-dimensional cooling channel property is initially assigned to the channels, after which they are converted into beam elements. This modeling choice significantly reduces computational cost while avoiding the complexity associated with fully meshed three-dimensional cooling channels. The cooling system mesh was generated using an automatic sizing strategy, since the channel dimensions vary from one iteration to another. Specifically, the parameter *Edge-Length Ratio Circuits* was set to 2.5. The inlet and outlet locations for the coolant were automatically defined based on the coordinates of the channels generated in Fusion 360. Water was selected as the coolant, with an inlet temperature fixed at 50 °C and a Reynolds number set to 15,000 to ensure efficient convective heat transfer. The box-shaped part and the sprue were then imported into Moldflow, and a Cool analysis was defined. The material was selected from the Moldflow database as *Generic ABS – Generic Shrinkage Characterised Material*. The shear viscosity of the melt is described in Moldflow using the Cross–WLF model, which accounts for the combined effects of shear rate, temperature, and pressure on the polymer viscosity. The viscosity η is expressed as (Eq.3):

$$\eta = \frac{D_1 . e^{\frac{-A_1(T-T^*)}{A_2+(T-T^*)}}}{1+\left(\frac{D_1 . e^{\frac{-A_1(T-T^*)}{A_2+(T-T^*)}} . \dot{\gamma}}{\tau^*}\right)^{1-n}} \quad (3)$$

where $T^* = D_2 + D_3 . p$, $A_2 = A_3 + D_3 . p$, T is the melt temperature, p is the pressure and $\dot{\gamma}$ the shear rate. The parameters D_1, D_2 , D_3, A_1, A_2 , n and τ^* are material-specific coefficients provided in the Moldflow database. The values corresponding to the selected ABS grade are reported in Table 1.

Table 1 The Cross-WLFparameters of the injection molded polymer

Parameter	D_1[Pa.s]	D_2 [K]	D_3 [K/Pa]	A_1	A_2 [K]	n	τ^* [Pa]
Value	2.8e+12	373.15	1.2e-07	27.76	51.6	0.37	15701.5

After meshing the part and the sprue, a melt temperature of 230°C was set up and a fixed total cycle time of 30 s (including injection, packing, and cooling phases) was imposed. The cooling time was deliberately not left to automatic determination by Moldflow, in order to prevent variations in cooling duration between different iterations and to ensure a consistent comparison among different cooling system designs. Although cooling time could be introduced as an additional design variable within the optimization framework, it was intentionally kept constant in order to isolate the influence of cooling system geometry on thermal uniformity and warpage. Allowing cooling time to vary for each configuration would increase computational cost and potentially mask the true effect of geometric modifications, since longer cooling durations could compensate for suboptimal cooling layouts.
Once the simulation was completed, the temperature distribution within the part was exported. The output provides the temperature value at each node and for each time step. The temperature field at the end of the cooling phase (30 s) was used to compute the average temperature and the standard deviation of the temperature within the part. This value was then transferred to the optimization platform and stored as an output variable directly associated with the second objective function representing temperature uniformity. The local cooling rate and temperature gradients within the part are determined by the interaction of the cooling channel geometry and material thermal properties. While coolant flow rate and temperature were fixed, the effective cooling experienced by the part is modulated by the cooling system geometry, which controls local heat extraction and thermal gradients. The standard deviation of the part temperature inherently reflects these variations in cooling rate and thermal uniformity.
Step 2: Geometric Optimization for Warpage Reduction: Once the optimal cooling system configuration was identified in Step 1, a second optimization step was carried out to further reduce part warpage through a controlled geometric modification of the component. This step focuses on the addition of a reinforcing border to the box-shaped part, a well-established strategy in injection molding of thin-walled box-like components to increase structural stiffness and mitigate deformation induced by differential shrinkage. The addition of reinforcing borders is known to be effective in reducing warpage, as increased section stiffness limits bending and out-of-plane deformation during cooling. However, excessively large or massive borders are not desirable in industrial practice. Oversized borders negatively affect the aesthetic appearance of the component, increase material consumption, and lead to higher part weight and production cost. Moreover, unnecessary material accumulation may alter cooling behavior and prolong cycle time, counteracting process efficiency objectives. For these reasons, the geometric reinforcement must be carefully designed to achieve sufficient warpage reduction while minimizing material usage and preserving the overall functional and visual characteristics of the part. The reinforcing border geometry, illustrated in Figure 4, is defined by three main dimensions: the border width L, representing the outward extension of the border from the box wall; the border height H, corresponding to the vertical extension of the border; and the border thickness T_h. The thickness T_h is generated in the CAD model by applying a hollowing operation (thicken feature in Fusion 360), ensuring a consistent wall structure. To guarantee that the

border thickness remains physically meaningful and does not exceed the border width, a dimensionless parameter "*b*" was introduced, such that (Eq.4):

$$T_h = b \times L \quad (4)$$

In the optimization problem, the border width L and height H were selected as primary design variables and varied within the range 5–20 mm. The dimensionless factor b was varied between 0.2 and 1.0. A value of ($b = 1$) corresponds to a fully solid border (i.e., ($T_h = L$)), while lower values of b generate hollow borders with reduced material usage.

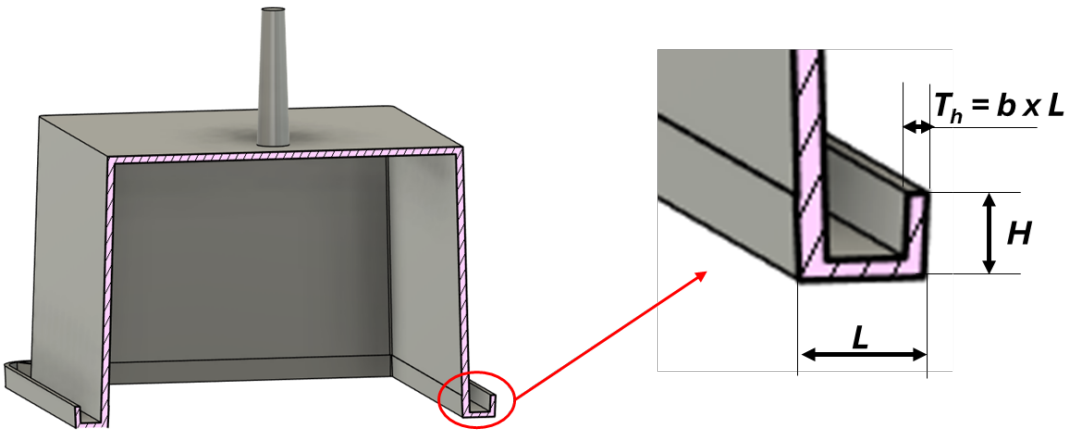

Fig. 3 Geometric parameters of the reinforcing border used for warpage reduction: border width (L), height (H), and thickness (T_h), with T_h defined as $T_h = b \times L$.

The objective of the second optimization step is twofold. The primary objective is the minimization of the maximum deflection of the molded part, which is used as a quantitative indicator of warpage severity. In parallel, a second objective is introduced to minimize the total volume of the molded box, thereby limiting material consumption and avoiding excessive geometric reinforcement. This multi-objective formulation enables the identification of border configurations that provide effective warpage reduction with minimal material penalty.

The optimization workflow implemented in Step 2 closely follows the structure adopted in Step 1. For each iteration, the optimization algorithm generates a new set of design variables (L , H, and b), which are automatically assigned to a parametric CAD model in Autodesk Fusion 360. The updated geometry of the reinforced box is then exported in STEP format, and the total volume of the part is computed and written to an output file. This value is subsequently read by the optimization platform and assigned to the objective function related to volume minimization.

The generated STEP file is then imported into Autodesk Moldflow, where the simulation is automatically configured. The cooling system used in this second optimization step corresponds to the optimal configuration identified in Step 1, ensuring that the thermal conditions remain fixed and that the effects of geometric modification on warpage can be isolated. All process parameters, including melt temperature, injection time, packing time and pressure, and total cycle time, were kept constant for all iterations. The melt temperature (230 °C) and mold temperature (60 °C) were selected according to the recommended processing window provided in the material datasheet. The injection time was fixed at 4 s; this value was determined through preliminary "Fill" simulations in Autodesk Moldflow to ensure complete cavity filling under all geometric configurations prior to launching the optimization procedure. Although the proposed optimization framework allows process parameters to be treated as additional design variables, they were intentionally kept constant in this study in order to isolate the influence of the reinforcing border geometry on warpage reduction. Introducing variable processing conditions would significantly increase computational cost and obscure the specific contribution of geometric modification.

After completion of the simulation, the maximum deflection of the part is extracted from the Moldflow results and assigned to the objective function representing warpage minimization. Under

these fixed processing conditions, the predicted injection pressures remained within a narrow range (approximately 40–60 MPa), with minor variations attributable to changes in effective thermal conditions and border geometry.

Results and Discussion

Figure 4 presents the two-dimensional scatter plot obtained at the end of the multi-objective optimization procedure for the cooling system design. Each point in the diagram represents a feasible cooling system configuration evaluated during the optimization process. The horizontal axis reports the total length of the cooling channels, L_{tot}, while the vertical axis reports the standard deviation of the temperature within the molded part at the end of the cooling phase, σ_T. A clear clustering of solutions can be observed, with the population organized into six distinct groups. Each group corresponds to a fixed value of the design variable n_1, representing the number of branches from which baffles are introduced in the moving plate. Within each group, variations in channel diameter d_c and distance factor a generate solutions with comparable total channel lengths and temperature standard deviations. As expected from a physical standpoint, increasing the number of baffle branches n_1 leads to a systematic increase in the total cooling channel length. At the same time, a monotonic reduction in the temperature standard deviation within the part is observed. This trend confirms the effectiveness of baffles in enhancing heat extraction from the inner regions of the box-shaped component, thereby reducing the thermal gradient between inner and outer surfaces and promoting a more homogeneous temperature distribution.

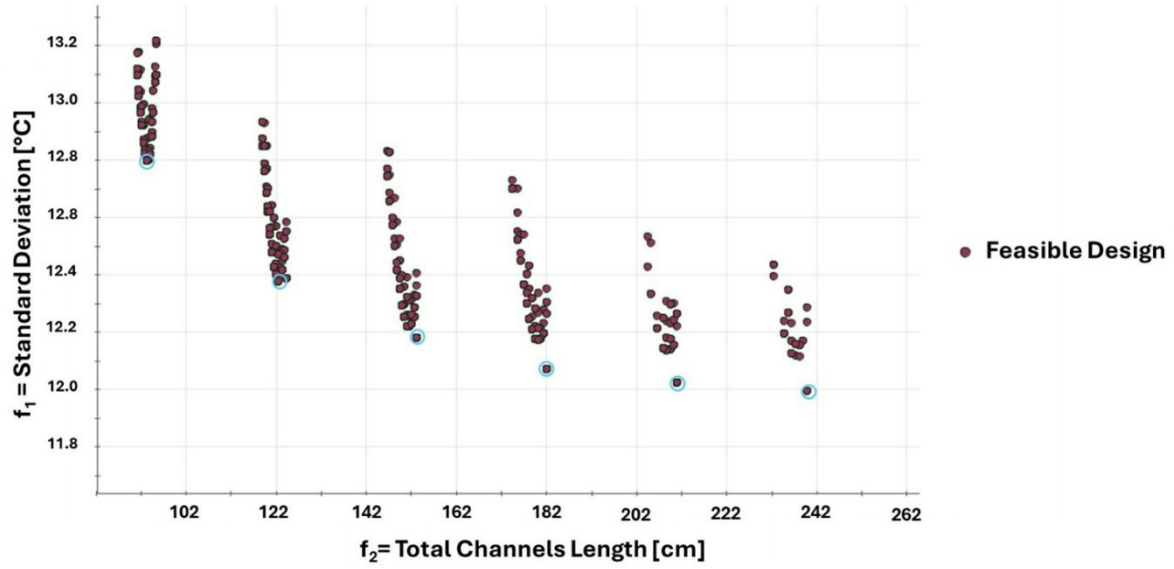

Fig. 4 Two-dimensional scatter plot obtained at the end of the multi-objective optimization procedure for the cooling system design.

For each group of solutions corresponding to a fixed value of the number of baffle branches n_1, the configuration exhibiting the minimum temperature standard deviation represents the best-performing design in terms of thermal uniformity, as it dominates all other solutions within the same group by achieving a lower σ_T without increasing the total cooling channel length. When these best-performing configurations are compared across different values of n_1, none of them dominates another, since improvements in temperature uniformity are systematically obtained at the expense of increased cooling system length. As a result, these configurations are non-dominated with respect to the two competing objectives of minimizing the temperature standard deviation σ_T and the total cooling channel length L_{tot}, and they form a discrete approximation of the Pareto front. These Pareto-optimal solutions are highlighted in blue in Figure 4 and summarized in Table 2. It can be observed that the distance factor a equals 1 for all Pareto-optimal solutions. This does not mean that the parameter was fixed; rather, the optimization converged to the lower bound of its admissible range (1–2.5),

indicating that positioning the cooling plane as close as allowed to the part improves thermal performance within the considered design space.

Table 2 Pareto-optimal cooling designs versus initial design

Design ID	Total channels length [cm]	Temperature standard deviation [°C]	d_c [mm]	a	n_l [mm]
0 (before optimization)	34.1	22.1	12	1	0
101	93.1	12.8	14	1	3
12	122.3	12.3	12	1	4
125	152.9	12.2	8	1	5
156	181.8	12.1	8	1	6
183	210.7	12.0	8	1	7
818	239.5	11.9	8	1	8

It is important to highlight that the introduction of baffles leads to a substantial reduction in temperature standard deviation compared to the initial configuration (22.1°C), with all Pareto-optimal solutions exhibiting values close to 12°C. The differences of approximately 1°C observed among Pareto-optimal designs therefore correspond to incremental refinements within an already significantly improved thermal regime. In this context, the optimization primarily captures the trade-off between marginal gains in thermal uniformity and the associated increase in cooling system length. Among these Pareto-optimal solutions, Design ID 818 achieves the lowest temperature standard deviation, corresponding to the most uniform temperature distribution within the part. However, this improvement is obtained at the expense of a significantly increased cooling system length, which may negatively impact mold structural integrity and manufacturing cost. Considering the trade-off between thermal performance and cooling system complexity, Design ID 12 was selected as the optimal compromise solution. Compared to Design ID 818, the total cooling channel length is reduced by approximately 49%, while the increase in temperature standard deviation remains limited. This configuration therefore achieves a substantial homogenization of the temperature field with a considerably more compact and manufacturable cooling system.

Overall, the results of Step 1 demonstrate that the number of baffle branches is the dominant parameter governing temperature uniformity in the considered design space, and that a balanced cooling system configuration can be identified through multi-objective optimization by explicitly accounting for both thermal performance and practical manufacturing constraints.

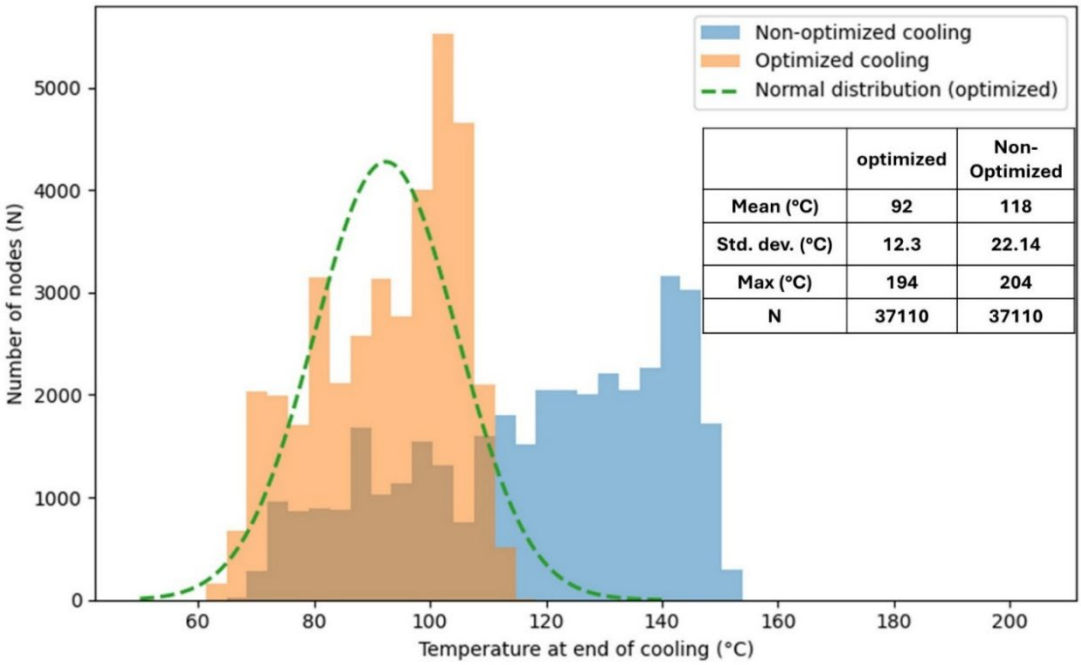

Fig. 5 Comparison of nodal temperature distributions at the end of cooling for the reference and optimized cooling systems, showing improved thermal uniformity with baffles.

Figure 5 compares the temperature distributions within the molded part at the end of the cooling phase for the non-optimized reference cooling system (without baffles) and the optimized cooling configuration selected from the Pareto front. The distributions are represented in terms of histograms of nodal temperatures, together with the main statistical indicators. In the reference configuration without baffles, the temperature field exhibits a wide dispersion, characterized by a large standard deviation and the presence of pronounced high-temperature regions. This behavior reflects the limited ability of the conventional cooling layout to extract heat from the inner regions of the box-shaped component, resulting in significant thermal gradients between the inner and outer surfaces. After optimization, a substantial improvement in thermal uniformity is observed. The standard deviation of the temperature distribution decreases from 22.1 °C to 12.3 °C, corresponding to a reduction of approximately 44%. In addition to this quantitative improvement, the optimized cooling system produces a markedly more compact and symmetric temperature distribution, with a significant reduction in extreme temperature values. For the optimized cooling configuration, the temperature distribution becomes narrower and more regular. When compared with a normal distribution, a good qualitative agreement is observed. Although no assumption of strict normality is imposed, the absence of pronounced hot or cold regions indicates a more homogeneous thermal state of the part at the end of the cooling phase. This improvement in temperature homogenization is directly linked to the presence of baffles in the moving plate, which enhance heat extraction from the inner surfaces of the component and reduce differential cooling. The resulting reduction in temperature gradients is expected to significantly mitigate non-uniform shrinkage during solidification and, consequently, contribute to a reduction in warpage. These results confirm the effectiveness of the first optimization step in addressing the thermal root cause of deformation in thin-walled box-shaped parts.

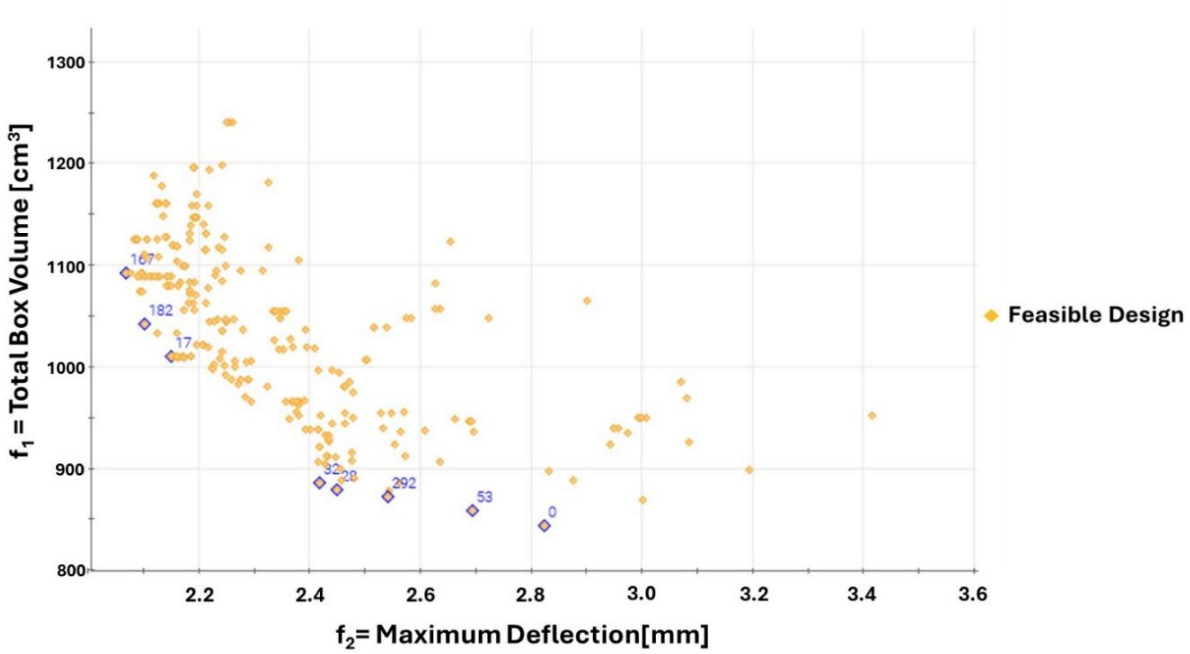

Fig.6 Scatter plot of maximum part deflection versus total volume for reinforced box designs, showing the trade-off between warpage reduction and material usage.

Figure 6 presents the two-dimensional scatter plot obtained at the end of the second optimization step, illustrating the relationship between maximum part deflection and total part volume for the reinforced box configurations. Each point represents a feasible design evaluated during the multi-objective optimization and corresponds to a specific combination of the border design variables (L, H, b). The horizontal axis reports the maximum deflection of the part, used as a quantitative indicator of warpage, while the vertical axis reports the total volume of the molded box.

The distribution of solutions shows a wide variability in performance, with several configurations exhibiting simultaneously high deflection and high volume, indicating inefficient geometric reinforcement. In contrast, a subset of non-dominated solutions defines a Pareto-optimal region (highlighted in blue), where reductions in warpage are obtained only at the expense of increased material usage. This Pareto-optimal trade-off highlights the necessity of balancing geometric stiffness and material efficiency when designing reinforcing borders for warpage mitigation. The final design was selected from the Pareto-optimal solutions by balancing warpage reduction and material efficiency. Design ID 167 was chosen, as it exhibits the minimum maximum deflection among all evaluated configurations, equal to 2.06 mm, indicating the most effective mitigation of warpage. The corresponding total part volume is 1094.3 cm³, which remains moderate compared to other designs. Configurations with larger volumes, reaching up to 1242 cm³, do not provide further improvements in deflection and are therefore dominated. Conversely, designs with minimal volume (approximately 846 cm³) show a significant increase in deflection, up to 2.82 mm, reflecting insufficient structural stiffness. Design ID 167 thus represents the most efficient compromise between geometric reinforcement and material usage and was selected as the final optimized box configuration.

Figure 7 presents a comparative visualization of the warpage results obtained for three representative configurations, highlighting the progressive effectiveness of the proposed two-step optimization strategy. Figure 7a) shows the deformation field of the original box molded with the non-optimized cooling system, which exhibits a maximum deflection of 14.5 mm, indicative of severe warpage caused by pronounced thermal gradients and limited structural stiffness. Figure 7(b) reports the deformation of the original box geometry molded with the optimized cooling system identified in Step 1. In this case, the maximum deflection is significantly reduced to 3.12 mm, demonstrating the strong impact of cooling system optimization and temperature homogenization on warpage mitigation. Finally, Figure 7(c) illustrates the deformation of the geometrically optimized box molded with the optimized cooling system. The maximum deflection is further reduced to 2.06 mm, confirming the additional benefit provided by the reinforcing border once thermal non-uniformities

have been minimized. The comparison clearly shows that while cooling system optimization addresses the primary thermal cause of warpage, the combined application of optimized cooling and targeted geometric reinforcement enables the most effective reduction of deformation, resulting in an overall warpage reduction of more than 85% compared to the initial configuration.

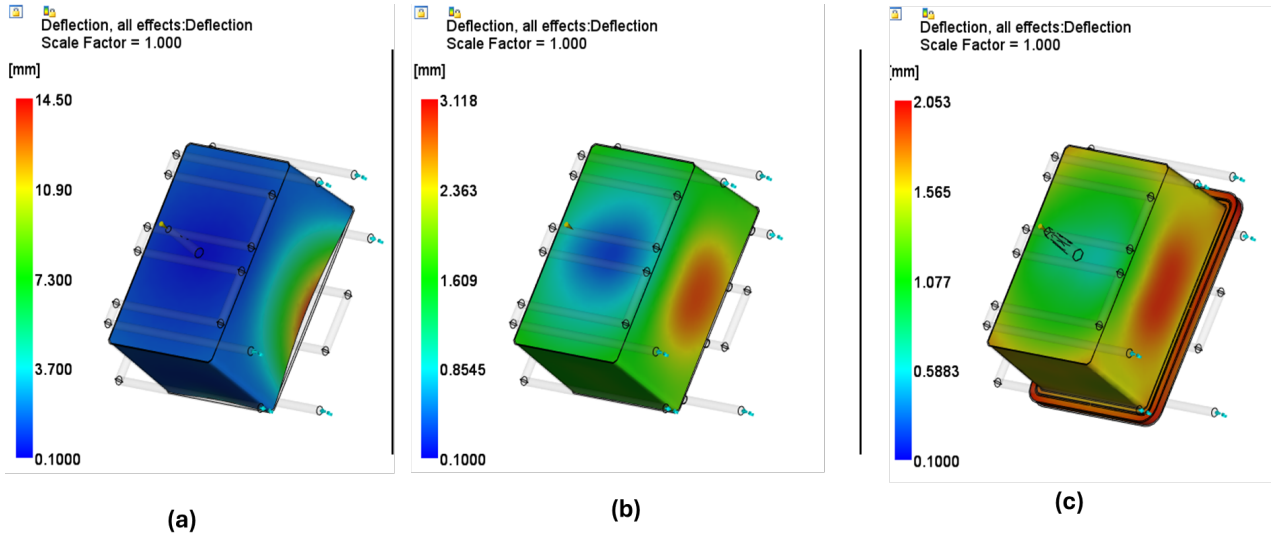

Fig.7 Comparison of warpage in three configurations: (a) non-optimized, (b) optimized cooling, and (c) optimized cooling with reinforced border, showing progressive reduction in maximum deflection.

Summary

This study presented a two-step optimization strategy for reducing warpage in thin-walled box-shaped injection-molded parts by jointly addressing thermal and geometric causes of deformation. In the first step, a multi-objective optimization of the mold cooling system, based on the integration of parametric CAD modeling, numerical simulation, and genetic algorithms, led to a substantial improvement in temperature uniformity through the optimized use of baffles. The second step further reduced warpage by introducing a controlled geometric reinforcement, optimized to balance structural stiffness and material efficiency. The combined application of optimized cooling and targeted border design resulted in an overall warpage reduction exceeding 85% compared to the initial configuration, while maintaining a compact and manufacturable design. The proposed methodology demonstrates the effectiveness of sequential, physics-driven optimization for improving part quality in injection molding and provides a systematic framework applicable to complex industrial components.

Fundings

This work was supported by the Emilia-Romagna Region, Italy [PR-FESR 2021-2027 -Priorità 1 - obiettivo specifico 1.1 - Azione 1.1.2 - Progetto “CUP E17G22001630003- SAFER. This work was also supported by PNRR–M4C2INV1.5, NextGenerationEU-Avviso 3277/2021-ECS_00000033-ECOSISTER-spk3.

References

[1] Q. Jiang, H. Liu, Q. Xiao, S. Chou, A. Xiong, H. Nie, Three-dimensional numerical simulation of total warpage deformation for short-glass-fiber-reinforced polypropylene composite injection-molded parts using coupled FEM, Journal of Polymer Engineering 38 (2018) 493–502. https://doi.org/10.1515/polyeng-2016-0445.

[2] T. Schrank, M. Berer, B. Haar, B. Ramoa, T. Lucyshyn, M. Feuchter, G. Pinter, V. Speranza, R. Pantani, Injection Molding Simulation of Polyoxymethylene Using Crystallization Kinetics Data and Comparison with the Experimental Process, Polymer Crystallization 2022 (2022) 1–15. https://doi.org/10.1155/2022/2387752.

[3] G. Zaniboni, K. Oubellaouch, R. Pelaccia, V. Siciliani, L. Orazi, B. Reggiani, Optical scanning application for numerical calibration of strain analysis on injection molded rail fastening components, in: 2025: pp. 2426–2535. https://doi.org/10.21741/9781644903599-262.

[4] K. Oubellaouch, R. Pelaccia, L. Orazi, P. Pozzi, S. Carmignato, N. Bonato, L. Donati, L. Raimondi, B. Reggiani, A novel experimental–numerical procedure for the rheological characterization of thermoplastic polymers applied to injection molding, Int J Adv Manuf Technol 140 (2025) 5419–5433. https://doi.org/10.1007/s00170-025-16522-7.

[5] N. Zhao, J. Lian, P. Wang, Z. Xu, Recent progress in minimizing the warpage and shrinkage deformations by the optimization of process parameters in plastic injection molding: a review, The International Journal of Advanced Manufacturing Technology 120 (2022) 85–101. https://doi.org/10.1007/s00170-022-08859-0.

[6] K. Oubellaouch, M. Sorgato, B. Reggiani, A Two-Step Simulation Approach to Predict Surface Micro-textures Replication in Injection-Molded Polymeric Parts, in: L. Fratini, L.M. Galantucci, L. Settineri (Eds.), Selected Topics in Manufacturing, Springer Nature Switzerland, Cham, 2025: pp. 157–173. https://doi.org/10.1007/978-3-031-99501-9_10.

[7] K. Oubellaouch, R. Pelaccia, N. Bonato, N. Bettoni, S. Carmignato, L. Orazi, L. Donati, B. Reggiani, Assessment of fiber orientation models predictability by comparison with X-ray μCT data in injection-molded short glass fiber-reinforced polyamide, The International Journal of Advanced Manufacturing Technology 130 (2024) 4479–4492. https://doi.org/10.1007/s00170-024-12990-5.

[8] M.A. Ali, N. Idayu, M.S.A. Aziz, M. Hadzley, Optimisation of process parameters in linear runner family injection mold using moldflow simulation software, I SSN 11 (2016).

[9] L. Zhang, T.-L. Chang, C.-C. Tsao, K.-C. Hsieh, C.-Y. Hsu, Analysis and optimization of injection molding process on warpage based on Taguchi design and PSO algorithm, Int J Adv Manuf Technol 137 (2025) 981–988. https://doi.org/10.1007/s00170-025-15099-5.

[10] F. Liu, J. Pang, Z. Xu, Multi-Objective Optimization of Injection Molding Process Parameters for Moderately Thick Plane Lens Based on PSO-BPNN, OMOPSO, and TOPSIS, Processes 12 (2023) 36. https://doi.org/10.3390/pr12010036.

[11] Y. Gao, X. Wang, Surrogate-based process optimization for reducing warpage in injection molding, Journal of Materials Processing Technology 209 (2009) 1302–1309. https://doi.org/10.1016/j.jmatprotec.2008.03.048.

[12] S. Taghizadeh, A. Özdemir, O. Uluer, WARPAGE PREDICTION IN PLASTIC INJECTION MOLDED PART USING ARTIFICIAL NEURAL NETWORK, 37 (2013).

[13] A. Gaspar-Cunha, J.B. Melo, T. Marques, A. Pontes, A Review on Injection Molding: Conformal Cooling Channels, Modelling, Surrogate Models and Multi-Objective Optimization, (2025). https://doi.org/10.20944/preprints202503.1555.v1.

[14] B.-O. Rhee, C.-S. Park, H.-K. Chang, H.-W. Jung, Y.-J. Lee, Automatic generation of optimum cooling circuit for large injection molded parts, Int. J. Precis. Eng. Manuf. 11 (2010) 439–444. https://doi.org/10.1007/s12541-010-0050-z.

[15] G. Wagner, J.M. Nóbrega, Conformal Cooling Channels in Injection Molding and Heat Transfer Performance Analysis Through CFD—A Review, Energies 18 (2025) 1972. https://doi.org/10.3390/en18081972.